

Electronic Supplementary Information (ESI)

Yield-prediction models for efficient exfoliation of soft layered materials into nanosheets

Kyohei Noda,^a Yasuhiko Igarashi,^{b,c} Hiroaki Imai,^a Yuya Oaki*^{a,c}

^a Department of Applied Chemistry, Faculty of Science and Technology, Keio University, 3-14-1 Hiyoshi, Kohoku-ku, Yokohama 223-8522, Japan

^b Faculty of Engineering, Information and Systems, University of Tsukuba, 1-1-1 Tennodai, Tsukuba 305-8573, Japan

^c JST, PRESTO, 4-1-8 Honcho, Kawaguchi, Saitama 332-0012, Japan

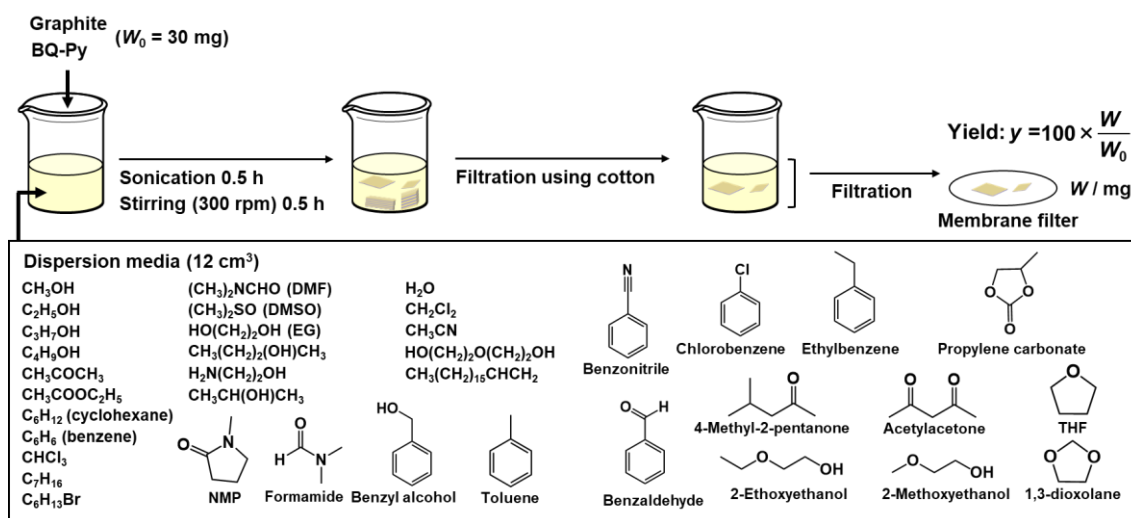
E-mail: oakiyuya@aplc.keio.ac.jp

Contents

Experimental methods (Scheme S1)	P. S2
List of all the explanatory variables (Table S1)	P. S4
Structure of the layered BQ-Py polymer (Fig. S1)	P. S6
List of the predicted yields (Table S2)	P. S7
Precursor layered materials and their exfoliation (Fig. S2)	P. S8
Dataset for ES-LiR (Tables S3)	P. S9
Additional TEM and AFM images of the nanosheets (Fig. S3)	P. S10
Consistency of the extracted descriptors in the revised model	P. S12
List of the D, P, and H values for preparation of the mixed solvents (Table S4)	P. S13
Summary of previous works about high-yield syntheses of 2D materials (Table S5)	P. S14

Experimental methods

Precursor layered materials. Graphite powder (Fujifilm-Wako, 98.0 %) was used as purchased. The layered BQ-Py polymer was synthesized by the method according to our previous report.⁸ Briefly, pyrrole (Py, TCI, 99.0 %) liquid and *p*-benzoquinone (BQ, TCI, 99.0 %) powder separately filled in the small vials were set in the larger vessel. Then, the vessel was maintained at 60 °C for 48 h. The powder in the bottle containing BQ was collected and then washed with acetone and 1-methyl-2-pyrrolidone. The resultant powder was dried under vacuum at 190 °C for 16 h.



Scheme S1. Experimental procedure and dispersion media for the exfoliation.^{7d,e}

Exfoliation. Graphite and BQ-Py powder (30 mg) were dispersed in 12 cm³ of following organic media (Scheme S1): methanol (99.8 %, Kanto), ethanol (Wako, 99.0 %), 1-propanol (Kanto, 99.5 %), 1-butanol (Kanto, 99.0 %), acetone (Kanto, 99.5 %), ethyl acetate (Kanto, 99.5 %), cyclohexane (Kanto, 99.7 %), benzene (Kanto, 99.5 %), chloroform (Kanto, 99.0 %), heptane (Kanto, 99.0 %), 1-bromohexane (Kanto, 99.0 %), *N,N*-dimethylformamide (DMF, Kanto, 99.5 %), dimethyl sulfoxide (DMSO, Kanto, 99.0 %), ethylene glycol (Kanto, 99.5 %), 2-butanol (Kanto, 99.0 %), 2-aminoethanol (Kanto, 99.0 %), 2-propanol (Kanto, 99.5 %), purified water, dichloromethane (Kanto, 99.5 %), acetonitrile (Kanto, 99.5 %), diethylene glycol (Kanto, 99.5 %), 1-octadecene (Kanto, 90.0 %), 1-methyl-2-pyrrolidone (NMP, Kanto, 99.0 %), formamide (Kanto, 98.0 %), benzyl alcohol (Kanto, 99.0 %), toluene (Kanto, 99.5 %), benzonitrile (Wako, 98.0 %), chlorobenzene (Wako, 99.0 %), ethylbenzene (Wako, 98.0 %), propylene carbonate (TCI, 98.0 %), benzaldehyde (Kanto, 99.0 %), 4-methyl-2-pentanone (Kanto, 99.5 %), acetylacetone (Kanto, 99.5 %), tetrahydrofuran (Kanto, 99.5 %), 2-ethoxyethanol (Kanto, 98.0 %), 2-methoxyethanol (Kanto, 99.0 %), 1,3-dioxolane (TCI, 98.0 %). These solvents were used without purification. The dispersion liquids were sealed in 20 cm³ of a glass sample bottle. The sample bottle was sonicated at room temperature for 0.5 h in a sonic bath (Branson, Bransonic Model 2510) and then maintained at 60 °C for 0.5 h under

stirring around 300 rpm. In our previous work,^{S1} the yield of the nanosheets was quite low when no sonication was applied to the dispersion liquid during the exfoliation process. The sonication under mild condition was used to initiate the exfoliation in the present work. The bulky unexfoliated and aggregated particles were removed by filtration using a polyethylene absorbent cotton for medical use. The dispersed nanosheets were suctioned and collected with ethanol using a polytetrafluoroethylene membrane filter with 0.1 μm in the pore size. The weight of the filter was measured before collection of the nanosheets. The filter was washed with ethanol and then dried under vacuum. The initial weigh was measured. The weight of the filter with the nanosheets was measured after drying under vacuum. In this manner, the weight of the collected nanosheets (W) was measured. The actual yield (y) was calculated using (Eq. 2) by the initial weight of the precursor layered materials (W_0) and weight of the collected nanosheets (W).^{7d-f} Only the fractured smaller particles and/or nanosheets passed through the filter (Fig. S2). The major of the resultant nanosheets can be collected by the present method.

Structure characterization. The particle size of graphite and layered BQ-Py was measured by the images of scanning electron microscopy (JEOL JSM-7600F). The nanosheets were observed by atomic force microscopy (AFM, Shimadzu, SPM-9700HT) and transmission electron microscopy (TEM, FEI, Tecnai G2). The colloidal liquid containing the nanosheets was dropped on a cleaned silicon substrate for AFM and collodion membrane for TEM observations. The particle-size distribution of the resultant nanosheets in the dispersion liquids was analyzed by DLS (Otsuka Electronics, ELSZ-2000ZS).

Yield-prediction models. The predicted yield for exfoliation of graphite and BQ-Py was calculated using (Eq. 2) by the two descriptors x_{18} and x_{35} (Table S2). ES-LiR was carried out on the dataset in Table S3. Explanatory variables (x_n : $n = 2, 4, 5, 8, 10, 14, 16, 17, 18, 33,$ and 35 in Table S3) were calculated using the following softwares; ChemBio3D Ultra 13.0 (x_n : $n = 2$), Gaussian 16W by density functional theory (DFT) with B3LYP based on the 6–311G basis set (x_n : $n = 14, 33$), and Hansen Solubility Parameters in Practice (HSPiP, version 5.0.03) (x_n : $n = 16–18, 35$). The other parameters (x_n : $n = 4, 5, 8, 10$) were referred to database.^{7d-f} ES-LiR analysis and construction of the prediction models were carried out using Python.

Additional Reference

S1. R. Mizuguchi, H. Imai and Y. Oaki, *Nanoscale Adv.*, 2020, **2**, 1168.

List of all the explanatory variables

Table S1. List of the explanatory variables (x_n , $n = 1-35$).^{7d-f}

$n / -$		Parameters	Unit
1	Dispersion media	Molecular weight	g mol^{-1}
2		^b Molecular length	nm
3		^a Melting point	$^{\circ}\text{C}$
4		^a Boiling point	$^{\circ}\text{C}$
5		^a Density	g cm^{-3}
6		^a Relative permittivity	–
7		^a Vapor pressure	Torr
8		^a Viscosity	cP
9		^a Refractive index	–
10		^a Surface tension	mJ m^{-2}
11		^b Heat capacity	$\text{cal mol}^{-1} \text{K}^{-1}$
12		^b Entropy	$\text{cal mol}^{-1} \text{K}^{-1}$
13		^b Enthalpy	kcal mol^{-1}
14		^b Dipole moment	Debye
15		^b Polarizability	$10^{40} \text{C}^2 \text{m}^2 \text{J}^{-1}$
16		^b HSP dispersion	–
17		^b HSP polarity	–
18		^b HSP hydrogen bond	–
19	Interlayer guest	Molecular weight	–
20		^b Polarizability	$10^{40} \text{C}^2 \text{m}^2 \text{J}^{-1}$
21		^b Dipole moment	Debye
22		^b Heat capacity	$\text{cal mol}^{-1} \text{K}^{-1}$
23		^b Entropy	$\text{cal mol}^{-1} \text{K}^{-1}$
24		^b Enthalpy	kcal mol^{-1}
25		^b Molecular length	nm
26		^c Interlayer distance	nm
27		^c Composition of the guest	–
28		^{c,e} Interlayer density	g cm^{-3}
29		^b HSP dispersion	–
30		^b HSP polarity	–
31		^b HSP hydrogen bond	–
32		^a Guest-medium	^b Δ Polarizability ($x_{20}-x_{15}$)
33	^b Δ Dipole moment ($x_{21}-x_{14}$)		Debye
34	^b Δ Heat capacity ($x_{22}-x_{11}$)		$\text{cal mol}^{-1} \text{K}^{-1}$
35	^b HSP distance		–

^a Literature values. ^b Calculation values by commercial softwares. ^c Experimental values. ^d The data were calculated from the differences between the values of dispersion media and interlayer guests.

These explanatory variables were prepared for construction of the yield-prediction model in our previous work.^{7d,e} The yield-prediction model (Eq. 1) was prepared for exfoliation of the layered composites consisting of the host transition-metal-oxide layers and interlayer organic guests in organic dispersion media, as shown in Fig. 1a. The physicochemical parameters about the interlayer guests, dispersion media, and their combinations were selected as the potential descriptors (Table S1).

In the present work, the interlayer guest was not introduced in the graphite and BQ-Py. The descriptors x_{18} and x_{35} are required for calculation of the yield using (Eq. 1). The descriptor x_{35}

(HSP-distance) was calculated by the differences in HSP (D, P, H) terms between graphite or BQ-Py and dispersion media (See Fig. S1 in the ESI).

For ES-LiR, the potential descriptors (x_n : $n = 2, 4, 5, 8, 10, 14, 16, 17, 18, 33$, and 35 in Table 2) were selected from Tables S1 on the basis of our experience and perspective to reduce the calculation cost. The descriptor x_{33} (Δ Dipole moment) was calculated by the differences in the dipole moment between graphite or BQ-Py and dispersion media.

Structure of the layered BQ-Py polymer

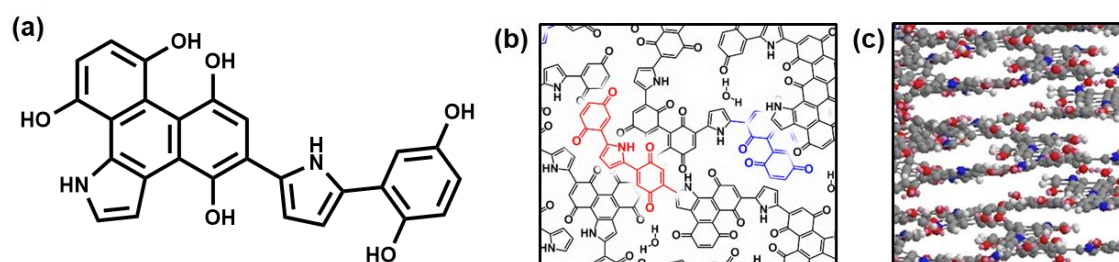


Fig. S1. Schematic models of the layered BQ-Py polymer.⁸ (a) Partial molecular structure for calculation of HSP D, P, and H terms. (b, c) Layered structures viewed in the vertical (b) and perpendicular (c) directions to the layers.

(D, P, H) terms were calculated to be (24.4, 6.1, 0.1) for the partial structure of the layered BQ-Py (Fig. S1a). BQ and Py were randomly copolymerized via the C-C bond formation and pericyclic reactions.⁸ Therefore, the random and quasi-2D network polymers were generated as shown in Fig. S2. As the network is not perfectly extended into the planar structure, the networks branched and overlapped in the vertical direction, as indicated with blue and red colors in Fig. S1b. The layered BQ-Py partially had the interlayer connections via the covalent bond (Fig. S1c). Therefore, the exfoliation provides not the monolayered nanosheets but the stacked nanosheets with the anisotropic morphology (Fig. 2g).

List of the predicted yields

Table S2. Estimated (y') and actual (y) yields for the predicted high- and low-yield conditions.

Predicted high-yield conditions (top)				Predicted low-yield conditions (bottom)			
Host	Graphite	Yield	Yield	Host	Graphite	Yield	Yield
Rank	Medium	$y' / \%$	$y / \%$	Rank	Medium	$y' / \%$	$y / \%$
1	1,3-Dioxolane	54.74	15.97	1	Hexane	-8.39	1.74
2	Benzyl alcohol	51.98	24.88	2	Heptane	-7.25	5.14
3	2-Methoxyethanol	51.41	14.94	3	Cyclohexane	-3.80	9.62
4	2-Ethoxyethanol	50.86	14.80	4	Octadecene	3.38	20.39
5	2-Aminoethanol	50.52	28.29	5	Benzene	5.80	0
	Average	51.90	19.78		Average	-2.05	7.38
	Standard deviation	1.50	5.68		Standard deviation	5.68	7.29
Host	BQ-Py	Yield	Yield	Host	BQ-Py	Yield	Yield
Rank	Medium	$y' / \%$	$y / \%$	Rank	Medium	$y' / \%$	$y / \%$
1	Benzyl alcohol	14.69	19.86	1	Hexane	-29.30	0
2	Benzaldehyde	11.62	25.72	2	Heptane	-26.81	3.28
3	Ethylene Glycol	9.88	14.55	3	Acetonitrile	-20.89	17.31
4	Chlorobenzene	5.97	23.04	4	Cyclohexane	-18.40	6.45
5	2-Methoxyethanol	5.80	22.04	5	4-methyl-2-pentanone	-12.10	14.62
	Average	9.59	21.04		Average	-21.50	8.33
	Standard deviation	3.40	3.75		Standard deviation	6.12	6.61

The predicted yields (y') were calculated using (Eq. 1). The prediction model (Eq. 1) was constructed in our previous work.^{7e} The layered composites of transition-metal oxides and interlayer organic guests were exfoliated in organic dispersion media. The training was carried out on the yield data. In the present work, the model was applied to the different types of the layered materials, such as graphite and BQ-Py. It is not easy to predict the accurate value of the yields precisely. Nevertheless, the high- and low-yield conditions have the significant differences.

Precursor layered materials and their exfoliation

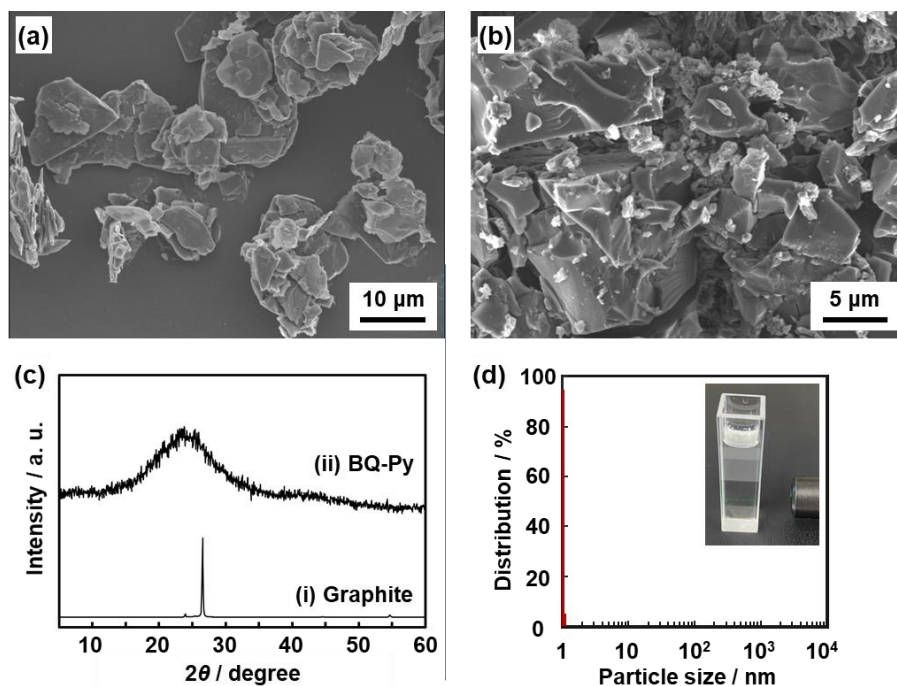


Fig. S2 (a,b) SEM images of the precursors graphite (a) and layered BQ-Py polymer (b). (c) X-ray diffraction patterns. (d) DLS chart and photograph (inset) of the dispersion liquid after the exfoliation of graphite in benzyl alcohol and subsequent collection of the nanosheets using filtration.

The average sizes of the primary particles were estimated from the SEM images (Fig. S2a,b). The primary particles form the aggregates. The layered materials with different crystallinity were used in the present work (Fig. S2c). According to the size of the precursor layered materials, the dispersion liquid containing the unexfoliated and exfoliated nanosheets was firstly filtered using cotton to remove the unexfoliated and aggregated materials. Then, the dispersed nanosheets were suctioned and collected using a membrane filter with 0.1 μm in the pore size. The weak Tyndall light scattering was observed on the filtered liquid (the inset of Fig. S2d). However, the DLS chart representing the size distribution was not obtained from the filtered liquid because the concentration is too low to analyze using light scattering (Fig. S2d). The fractured smaller particles and/or nanosheets passed through the filter. The facts indicate that the resultant nanosheets are collected by suction using the filter. The facts indicate that the resultant nanosheets are collected by suction using the filter. When the dried filter was inverted, the collected powder was not removed from the surface.

Dataset for ES-LiR

Table S3. Dataset of the yields in total 60 conditions for ES-LiR.

No.	host	Dispersion media	x_2	x_4	x_5	x_8	x_{10}	x_{14}	x_{16}	x_{17}	x_{18}	x_{33}	x_{35}	Yield / %
1	Graphite	1,3-Dioxolane	0.39	78.00	1.06	0.59	31.20	1.49	17.3	9.2	8.9	1.49	1.85	15.97
2	Graphite	Benzyl alcohol	0.70	205.41	1.04	5.58	38.25	2.06	18.4	6.3	13.7	2.06	6.76	24.88
3	Graphite	2-Methoxyethanol	0.65	124.50	0.97	1.71	33.30	0.34	16.4	9.2	15.8	0.34	8.71	14.94
4	Graphite	2-Ethoxyethanol	0.77	135.10	0.93	1.84	28.20	0.47	16.2	8.1	13.9	0.47	7.27	14.80
5	Graphite	2-Aminoethanol	0.53	171.10	1.01	18.95	48.89	1.22	17.8	10.3	21.3	1.22	13.64	28.29
6	Graphite	Ethanol	0.41	78.29	0.78	1.08	24.03	1.94	15.8	8.8	19.4	1.94	12.51	36.22
7	Graphite	DMF	0.42	153.00	0.94	0.80	37.10	4.37	17.4	13.7	11.3	4.37	5.81	36.53
8	Graphite	1-Propanol	0.54	97.15	0.80	1.95	25.26	1.84	15.7	6.8	17.4	1.84	11.02	32.42
9	Graphite	1-Butanol	0.67	117.25	0.81	3.00	27.18	1.88	16.0	5.7	15.8	1.88	7.39	2.71
10	Graphite	2-Propanol	0.44	82.40	0.79	2.04	22.90	1.93	15.5	7.2	12.8	1.93	7.44	22.99
11	Graphite	Chlorobenzene	0.55	132.00	1.11	0.81	35.97	2.53	18.7	3.6	3.5	2.53	7.22	25.86
12	Graphite	Acetonitrile	0.32	81.60	0.78	0.34	31.78	3.93	15.3	18.0	6.1	3.93	10.36	4.75
13	Graphite	1-Buromohexane	0.89	155.20	0.65	0.29	20.41	2.70	16.6	3.3	2.9	2.70	8.18	12.29
14	Graphite	Ethylbenzene	0.73	136.19	0.87	0.60	29.20	0.48	17.6	2.3	3.0	0.48	8.47	6.19
15	Graphite	Toluene	0.58	110.63	0.86	0.55	30.86	0.37	18.0	1.4	2.0	0.37	9.74	4.30
16	Graphite	Benzene	0.49	80.10	0.88	0.65	31.54	0	18.4	0	2.0	0	10.94	0
17	Graphite	Octadecene	2.34	179.00	0.79	3.60	28.49	0.45	15.9	0.9	1.5	0.45	11.25	20.39
18	Graphite	Cyclohexane	0.50	80.74	0.78	0.98	27.62	0	16.6	0.1	0.1	0	12.26	9.62
19	Graphite	Heptane	0.95	98.40	0.68	0.42	22.10	0.06	15.3	0	0	0.06	13.23	5.14
20	Graphite	Hexane	0.82	68.74	0.65	0.29	20.41	0	14.9	0	0	0	13.57	1.74
21	Graphite	Methanol	0.29	64.55	0.79	0.55	23.98	2.11	15.1	12.3	22.3	2.11	15.99	22.66
22	Graphite	Benzaldehyde	0.60	178.00	1.05	1.40	40.72	3.68	18.9	8.0	6.2	3.68	2.68	35.69
23	Graphite	THF	0.42	65.96	0.89	0.46	26.99	2.26	16.8	5.7	8.0	2.26	4.34	26.12
24	Graphite	Formamide	0.31	210.00	1.14	2.93	58.20	4.24	17.3	18.7	19.3	4.24	15.00	16.1
25	Graphite	DMSO	0.47	189.00	1.10	1.99	45.75	5.16	18.4	16.4	10.2	5.16	7.57	6.67
26	Graphite	Acetone	0.42	58.08	0.78	0.30	26.23	3.23	15.5	10.4	7.0	3.23	5.17	29.07
27	Graphite	Acetylacetone	0.62	140.50	0.98	0.82	31.20	1.63	17.0	11.0	6.8	1.63	2.77	42.42
28	Graphite	Diethylene glycol	0.86	245.00	1.11	32.00	46.97	2.34	16.0	6.0	6.7	2.34	5.28	6.90
29	Graphite	Water	0.15	99.97	1.00	0.89	72.59	2.43	15.5	16.0	42.3	2.43	35.60	2.88
30	Graphite	Ethyl acetate	0.64	77.11	0.89	0.43	26.26	4.95	15.8	5.3	7.2	4.95	5.97	18.82
31	BQ-Py	Benzyl alcohol	0.69	205.41	1.04	5.58	38.25	2.06	18.4	6.3	13.7	0.85	18.14	19.86
32	BQ-Py	2-Aminoethanol	0.53	171.10	1.01	18.95	48.89	1.22	17.8	10.3	21.3	1.69	25.32	9.23
33	BQ-Py	Benzaldehyde	0.60	178.00	1.05	1.40	40.72	3.68	18.9	8.0	6.2	0.77	12.72	25.72
34	BQ-Py	Ethylene glycol	0.51	197.85	1.11	23.50	48.40	0	17.8	13.5	27.4	2.91	31.21	14.55
35	BQ-Py	Chlorobenzene	0.55	132.00	1.11	0.81	35.97	2.53	18.7	3.6	3.5	0.38	12.16	23.04
36	BQ-Py	2-Methoxyethanol	0.65	124.50	0.97	1.71	33.3	0.34	16.4	9.2	15.8	2.57	22.63	22.04
37	BQ-Py	Ethanol	0.41	78.29	0.78	1.08	24.02	1.94	15.8	8.8	19.4	0.97	25.99	15.27
38	BQ-Py	1-Butanol	0.67	117.25	0.81	3.00	27.18	1.88	16.0	5.7	15.8	1.04	23.00	13.83
39	BQ-Py	2-Ethoxyethanol	0.77	135.10	0.93	1.84	28.20	0.47	16.2	8.1	13.9	2.44	21.53	17.64
40	BQ-Py	NMP	0.52	202.00	1.03	1.67	40.79	4.30	18	12.3	7.2	1.39	15.90	4.63
41	BQ-Py	Benzene	0.49	80.10	0.88	0.65	31.54	0	18.4	0	2.0	2.91	13.59	18.40
42	BQ-Py	Toluene	0.58	110.63	0.86	0.553	30.86	0.37	18.0	1.4	2.0	2.54	13.77	24.30
43	BQ-Py	Ethyl acetate	0.64	77.11	0.89	0.43	26.26	4.95	15.8	5.3	7.2	2.04	18.62	11.82
44	BQ-Py	1-Buromohexane	0.89	155.20	0.65	0.29	20.41	2.70	16.6	3.3	2.9	0.21	16.09	3.02
45	BQ-Py	Acetone	0.42	58.08	0.78	0.30	26.23	3.23	15.5	10.4	7.0	0.32	19.57	8.68
46	BQ-Py	4-methyl-2-pentanone	0.69	116.70	0.80	0.54	23.60	3.19	15.6	5.7	3.9	0.27	18.01	14.62
47	BQ-Py	Cyclohexane	0.50	80.74	0.78	0.98	27.62	0	16.6	0.1	0.1	2.91	16.71	6.45
48	BQ-Py	Acetonitrile	0.32	81.60	0.78	0.34	31.78	3.93	15.3	18.0	6.1	1.02	22.56	17.31
49	BQ-Py	Heptane	0.95	98.40	0.68	0.42	22.1	0.06	15.3	0	0	2.85	19.20	3.28
50	BQ-Py	Hexane	0.82	68.74	0.65	0.29	20.41	0	14.9	0	0	2.91	19.96	0
51	BQ-Py	Chloroform	0.29	61.18	1.48	0.54	29.87	1.53	17.8	3.1	5.7	1.38	14.65	2.43
52	BQ-Py	DMF	0.42	153.00	0.94	0.80	37.10	4.37	17.4	13.7	11.3	1.46	19.47	26.26
53	BQ-Py	DMSO	0.47	189.00	1.09	1.99	45.75	5.16	18.4	16.4	10.2	2.25	18.76	46.75
54	BQ-Py	benzonitrile	0.63	191.10	1.01	1.24	38.79	4.59	18.8	12.0	3.3	1.68	13.06	25.19
55	BQ-Py	THF	0.42	65.96	0.89	0.46	26.99	2.26	16.8	5.7	8.0	0.645	17.14	22.89
56	BQ-Py	dichloromethane	0.29	40.21	1.33	0.43	30.41	2.25	17.0	7.3	7.1	0.66	16.42	2.57
57	BQ-Py	formamide	0.31	210.00	1.14	2.93	58.20	4.24	17.3	18.7	19.3	1.33	27.00	4.68
58	BQ-Py	methanol	0.29	64.55	0.79	0.55	23.98	2.11	15.1	12.3	22.3	0.81	29.62	3.19
59	BQ-Py	2-butanol	0.52	98.50	0.80	4.20	24.53	1.85	15.7	5.8	12.3	1.06	21.25	26.62
60	BQ-Py	Water	0.15	99.97	1.00	0.89	72.59	2.43	15.5	16.0	42.3	0.48	46.86	11.10

New 40 yield data were added to the original 20 data in Table 1. This dataset was used for ES-LiR to validate the descriptors for yield prediction of soft layered materials stacked via van der Waals interaction. TEM and AFM observations were carried out on the samples No. 1, 2, 22, 31, 35, 55 in Table S3 to confirm the formation of the nanosheets.

Additional TEM and AFM images of the nanosheets

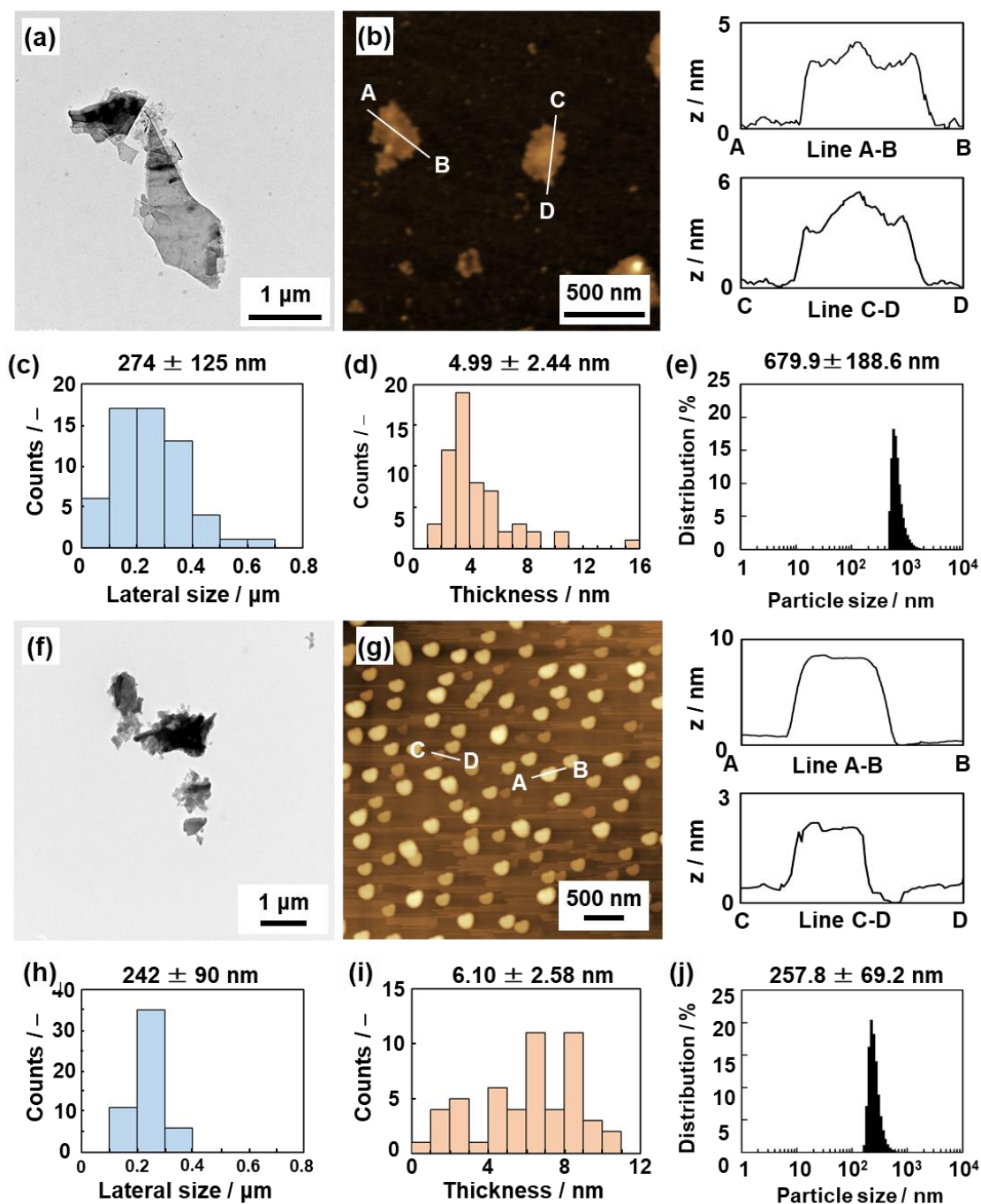


Fig. S3 Additional microscopy (a–d,f–i,k–n,p–s) and DLS (e,j,o,t) analyses of the graphite exfoliated in benzyl alcohol (a–e), BQ-Py exfoliated in benzyl alcohol (f–j), graphite exfoliated in benzaldehyde (k–o), and BQ-Py exfoliated in THF (p–t).

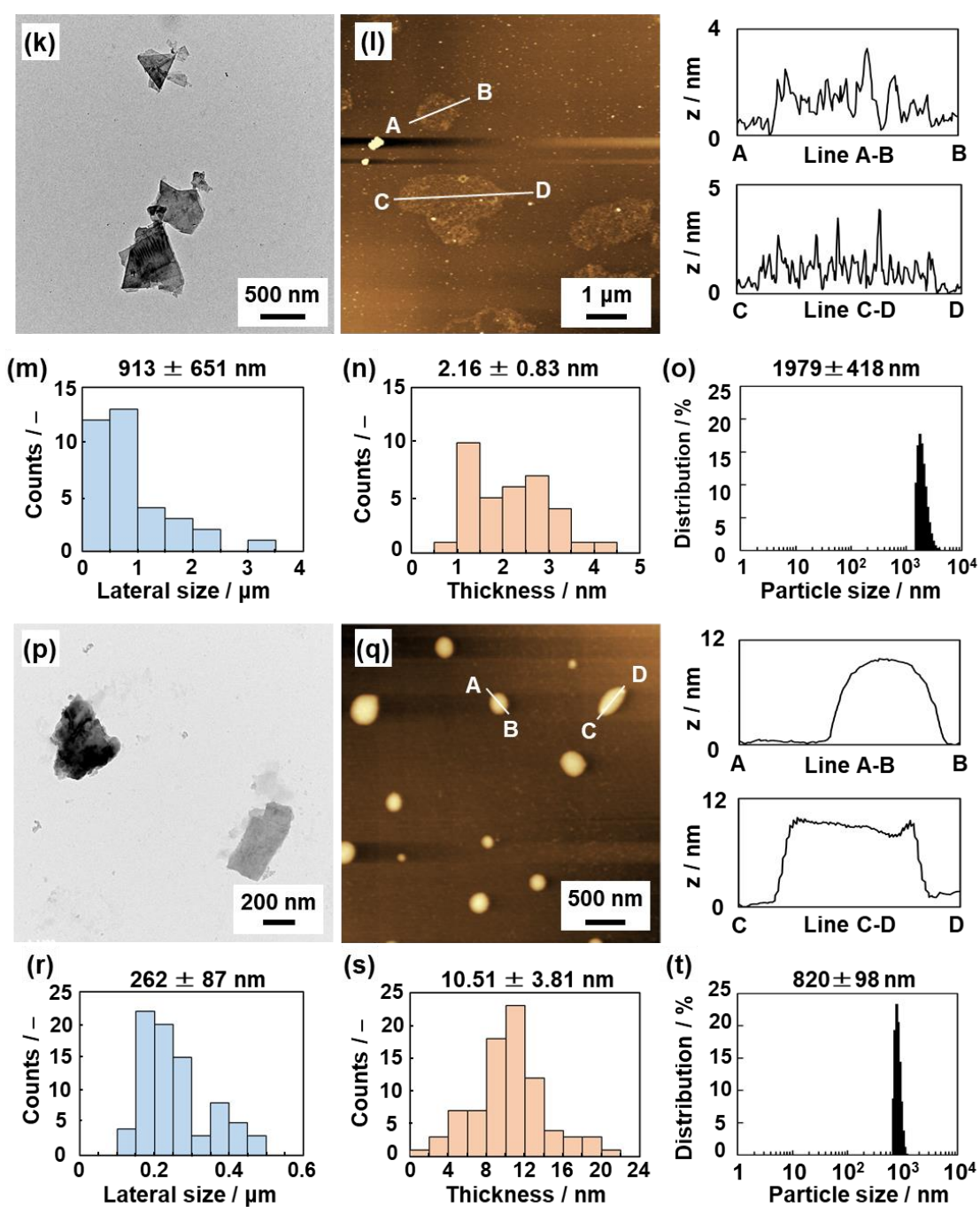


Fig. S3. (Continued)

These results support the formation of the nanosheets in No. 2, 22, 31, and 55 in Table S3. The same results for Entries 1 and 35 were displayed in Fig. 2 in the main text. These results indicate that exfoliation of graphite and layered BQ-Py provides the nanosheets.

Consistency of the extracted descriptors in the revised model

The correlation of the descriptors in the revised model (eq. 4) is explained as follows. The higher yield is achieved by the smaller x_{35} . The smaller HSP distance between the layers and dispersion media means their higher affinity. The positive correlation of x_{16} , x_{17} , and x_{18} indicates that the higher yield is achieved in dispersion media with the larger HSP D, P, H terms. The stronger interactions of the dispersion media to the host layers contribute to achieve the higher yield. The other potential factors, such as the size and crystallinity, can be included as the explanatory variables in the training dataset. The prediction model can be improved and expanded with addition of the yield data by the similar manner.

List of the D, P, and H values for preparation of the mixed solvents

Table S4. List of HSP distance for mixed solvent

Entry	Dispersion media	D	P	H	^a δD	^a δP	^a δH	HSP-d	Yield <i>y</i> / %
1	Chlorobenzene–DMF	18.05	8.65	7.4	0.05	−0.65	−0.3	0.72	48.01
2	1,3-Dioxolane–Benzaldehyde	18.1	8.6	7.55	0.1	−0.7	−0.15	0.74	41.09
3	Benzaldehyde–Acetylacetone	17.95	9.5	6.5	−0.05	0.2	−1.2	1.22	14.41
4	1,3-Dioxolane	17.3	9.2	8.9	0.7	0.1	−1.2	1.85	15.97
5	Benzaldehyde	18.9	8	6.2	−0.9	1.3	1.5	2.68	35.69
6	Acetylacetone	17	11	6.8	1	−1.7	0.9	2.77	42.42
7	THF	16.8	5.7	8	1.2	3.6	−0.3	4.34	26.12
8	Acetone	15.5	10.4	7	2.5	−1.1	0.7	5.17	29.07
9	Diethylene glycol	16	6	6.7	2	3.3	1	5.28	6.9
10	DMF	17.4	13.7	11.3	0.6	−4.4	−3.6	5.81	36.53
11	Ethyl acetate	15.8	5.3	7.2	2.2	4	0.5	5.97	18.82
12	Benzyl alcohol	18.4	6.3	13.7	−0.4	3	−6	6.76	24.88
13	Chlorobenzene	18.7	3.6	3.5	−0.7	5.7	4.2	7.22	25.86
14	2-Ethoxyethanol	16.2	8.1	13.9	1.8	1.2	−6.2	7.27	14.8
	Graphite	18.0	9.3	7.7					

^a δD, δP, and δH are the differences in the D, P, and H values of the dispersion media to those of graphite, respectively.

According to the D, P, and H values, the δD, δP, and δH values to graphite approach 0 with mixing the blue- and red-colored dispersion media in Table S4. The mixed solvents in Entries 1-3 have the smaller HSP-d compared with the pure solvents. The predicted yields of Entries 1-3 were 26.74, 26.64, and 26.27 %, respectively.

Summary of previous works about high-yield syntheses of 2D materials

Table S5. Summary of the synthetic time and yield in previous works.⁴

No.	Layered materials	Time / h	Yield / %	Ref.
1	Graphite	0.5	93	4a
2	Transition-metal dichalcogenide (TMD)	0.5	90	4b
3	TMD	0.5	58	4c
4	Graphite	1	95	4d
5	Graphite	1	48	This work

The high-yield syntheses were achieved in previous works.⁴ These works used the specific exfoliating agents and additives to promote the exfoliation into the monolayered and few-layered nanosheets. The present work studied the effects of the dispersion media on the yield. The prediction model can propose the appropriate liquid phase to induce the exfoliation efficiently.